A Framework for Discontinuous Fluctuation Distribution

M. E. Hubbard*

School of Computing, University of Leeds, Leeds, LS2 9JT, U.K.

SUMMARY

This paper describes a new numerical scheme for the approximation of systems of hyperbolic conservation laws. It generalises the fluctuation distribution framework by allowing the underlying representation of the solution to be discontinuous. Steady state numerical results are presented for the Euler equations of gasdynamics.
Copyright © 2000 John Wiley & Sons, Ltd.

KEY WORDS: Fluctuation distribution; Euler equations

1. INTRODUCTION

The concept of fluctuation distribution was originally proposed nearly 25 years ago [6] as a potential alternative to flux-based finite volume schemes for approximating hyperbolic conservation laws. Major advances during the intervening period have provided genuinely multidimensional schemes which can achieve very high orders of accuracy without spurious oscillations for both steady state and time-dependent scalar equations, along with generalisations to nonlinear systems of conservation laws. Details of both their foundations and some of the most important recent developments can be found in [7] (the reader is referred to the references therein for a full account). However, this has been matched by the progress of the finite volume approach, which has maintained its popularity for simulating flows of realistic complexity, largely due to its ability to provide plausible solutions in the most demanding of situations. Fluctuation distribution still lacks this robustness: its advantage is that when it does provide a sensible solution, it is typically more accurate, often by a significant margin, due its more realistic representation of multidimensional flow physics.

One of the strongest challenges to the dominance of finite volume schemes has been the emergence of the discontinuous Galerkin approach (see, for example [2, 7]). This allies the discontinuous, edge-based form associated with finite volumes (in which the conserved quantity within a control volume varies according to the net flux through the surface of that volume) with the continuous, cell-based form associated with finite elements (in which the conserved quantity associated with a test function varies according to the local flux variations). The

---

*Correspondence to: School of Computing, University of Leeds, Leeds, LS2 9JT, U.K.

resulting combination retains much of the robustness of finite volumes but is far more amenable to analysis and error estimation. Its local, discontinuous, nature also makes it simple to enhance using adaptive techniques (guided by the error analysis).

Fluctuation distribution does, however, have inherent advantages. Firstly, the most successful schemes have been designed to retain at a discrete level the most important underlying physical processes, and to do so in a genuinely multidimensional manner (a facility that the flux-based schemes cannot match). Secondly, because they use the fluctuations (which are related to the local flux *variations*, not the fluxes themselves) to predict the evolution of the conserved quantity, it becomes far simpler to discretise source terms which represent processes which have a natural balance with the fluxes. They are, in fact, very closely related to Petrov-Galerkin finite elements [1], but the change in viewpoint allows the inclusion of upwinding and the suppression of unphysical oscillations in a very natural manner.

Despite the advantages of the continuous representation of the solution used in the current framework for fluctuation distribution, it still has drawbacks, *e.g.* the application of h- and p-adaptivity and the construction of high order schemes which are free of numerically induced oscillations are hard to achieve. This paper seeks to address this issue by proposing a framework for fluctuation distribution in which the underlying representation of the solution is *discontinuous*. Unlike discontinuous Galerkin schemes the new approach will only use flux variations, not the fluxes, to update the conserved variable, though there is clearly a close relationship between the two. Results will be presented for steady state test cases involving the Euler equations of gasdynamics.

2. FLUCTUATION DISTRIBUTION

Consider the scalar conservation law given by

$$u_t + \vec{\nabla} \cdot \vec{f} \,=\, 0 \qquad \text{or} \qquad u_t + \vec{\lambda} \cdot \vec{\nabla} u \,=\, 0 \tag{1}$$

on a domain Ω, with appropriate initial conditions and boundary conditions imposed on the inflow part of $\partial\Omega$. Here $\vec{\lambda} = \partial\vec{f}/\partial u$ defines the advection velocity associated with the conservation law (1). This equation has an associated fluctuation which, for a triangular mesh cell $\triangle$ (for simplicity, the two-dimensional case will be considered from now on), is given by

$$\phi_c \,=\, -\int_{\triangle} \vec{\nabla} \cdot \vec{f} \, d\Omega \,=\, -\int_{\triangle} \vec{\lambda} \cdot \vec{\nabla} u \, d\Omega \,=\, \oint_{\partial\triangle} u \, \vec{\lambda} \cdot \vec{n} \, d\Gamma \,, \tag{2}$$

in which $\vec{n}$ represents the inward pointing unit normal to the cell boundary. When u is assumed to have a piecewise linear continuous representation with values stored at the mesh nodes, the discrete counterpart of ϕ_c is evaluated using an appropriate (conservative) linearisation [3, 7]. Ideally, this allows the integration in Equation (2) to be carried out exactly, giving

$$\phi_c \,=\, -S_{\triangle} \, \widetilde{\vec{\lambda}} \cdot \widetilde{\vec{\nabla} u} \,=\, -\frac{1}{2} \sum_{i \in \triangle} u_i \, \widetilde{\vec{\lambda}} \cdot \vec{n}_i \,, \tag{3}$$

where $S_{\triangle}$ is the cell area and the symbol $\widetilde{}$ indicates an appropriately linearised quantity. The index i loops over the vertices of $\triangle$ and $\vec{n}_i$ is the inward unit normal to the ith edge (opposite the ith vertex) multiplied by the length of that edge. This linearisation is straightforward for the cases considered in this paper [3, 7].

A simple forward Euler discretisation of the time derivative leads to an iterative update of the nodal solution values which is generally written as

$$u_i^{n+1} \; = \; u_i^n + \frac{\Delta t}{S_i} \sum_{j \in \cup \triangle_i} \alpha_i^j \, (\phi_c)_j \, , \tag{4}$$

where Δt is the time-step, S_i is the area of the median dual cell surrounding node i (one third of the total area of the triangles with a vertex at i), α_i^j is the distribution coefficient which indicates the appropriate proportion of the fluctuation $(\phi_c)_j$ to be sent from cell j to node i, and $\cup \triangle_i$ represents the set of cells with vertices at node i. Conservation is assured as long as $\sum_{i \in \triangle_j} \alpha_i^j \; = \; 1$, $\forall j$, where $\triangle_j$ represents the set of nodes at the vertices of cell j, $i.e.$ the whole of each fluctuation is sent to the nodes. The time derivative term in this construction is included here purely as a device for iterating to the steady state.

This framework has led to a range of upwind schemes, the most commonly used being the N scheme (oscillation-free but only first order accurate), the LDA scheme (allows arbitrary order accuracy at the expense of unphysical oscillations) and the PSI scheme (both free of unphysical oscillations and second order accurate, but tough to generalise to complex problems). Details of all of these schemes can be found in [7].

3. A DISCONTINUOUS SCHEME

A continuous representation of u was assumed throughout the discussion in Section 2. In this case, the integral of the conservation law (1) over Ω was divided between the mesh cells, leading to the fluctuations (2)/(3) which were used to update u, using (4), in a conservative manner. If the discrete representation of u is allowed to be discontinuous then

$$\int_\Omega \vec{\nabla} \cdot \vec{f} \, d\Omega \; = \; \sum_{j=1}^{N_c} \int_{\triangle_j} \vec{\nabla} \cdot \vec{f} \, d\Omega \; + \; \sum_{j=1}^{N_e} \int_{|_j} \vec{\nabla} \cdot \vec{f} \, d\Omega \, , \tag{5}$$

in which $|$ is used to represent a mesh edge (face in three dimensions) and N_c, N_e are the numbers of cells and edges, respectively. Each edge can be thought of as the limit of a rectangle as its width tends to zero, as illustrated on the left hand side of Figure 1, which leads to

$$\phi_e \; = \; -\lim_{\epsilon \to 0} \int_{\square_\epsilon} \vec{\nabla} \cdot \vec{f} \, d\Omega \; = \; \lim_{\epsilon \to 0} \oint_{\partial \square_\epsilon} \vec{f} \cdot \vec{n} \, d\Gamma \; = \; \int_| [\vec{f} \cdot \vec{n}] \, d\Gamma \, , \tag{6}$$

in which $[\;]$ represents the jump in a quantity across the edge, the sign of the difference being dictated by the direction chosen for $\vec{n}$. This is simply the integral along the interface of the flux difference across it. The discontinuous Galerkin approach would treat each flux term in this difference separately, first approximating it at the interface with an averaged "numerical" flux, and then sending its contribution to the evolution of the conservative variable to the mesh cell on the corresponding side of the interface. In this work ϕ_e is treated separately, as a fluctuation in a degenerate quadrilateral mesh cell.

Under the assumption that a conservative linearisation exists for the flux difference [5],

$$\phi_e \; = \; -\frac{1}{2} \sum_{k=1}^{N_q} w_k \, \widetilde{\vec{\lambda}}_k \cdot \vec{n} \, [u_k] \, , \tag{7}$$
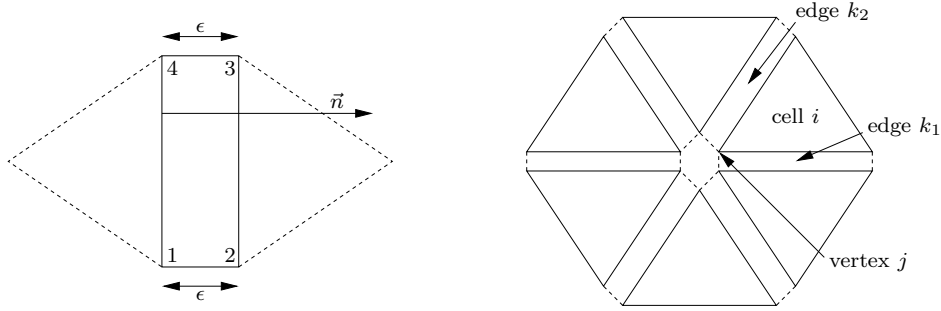
Figure 1. The mesh structure for the discontinuous fluctuation distribution at an edge (left) and around a node (right).

in which N_q is the number of quadrature points used, w_k are the weights and $\widetilde{\vec{\lambda}}_k = \partial \vec{f}(\tilde{u}_k)/\partial u$ ($\tilde{u}_k$ being a conservative average value for u at the specified quadrature point). For the equations considered here, Simpson's rule is accurate enough to integrate (6) exactly.

In order to ensure that these edge fluctuations can be used as part of a positive scheme, (7) is rewritten (using the numbering indicated on the left of Figure 1) as

$$\phi_e \;=\; \frac{1}{2}\widehat{\vec{\lambda}}_{12} \cdot \vec{n}\,(u_1 - u_2) \;+\; \frac{1}{2}\widehat{\vec{\lambda}}_{43} \cdot \vec{n}\,(u_4 - u_3), \tag{8}$$

in which the $\widehat{\vec{\lambda}}\ (\neq \widetilde{\vec{\lambda}})$ are given by

$$\widehat{\vec{\lambda}}_{12} \;=\; \frac{1}{3}\left(\vec{\lambda}_1 + \vec{\lambda}_2 + \frac{\vec{\lambda}_3 + \vec{\lambda}_4}{2}\right) \qquad \text{and} \qquad \widehat{\vec{\lambda}}_{43} \;=\; \frac{1}{3}\left(\vec{\lambda}_3 + \vec{\lambda}_4 + \frac{\vec{\lambda}_1 + \vec{\lambda}_2}{2}\right). \tag{9}$$

The fluctuation ϕ_e in (8) can now be distributed to the four cell vertices (two pairs of coincident vertices) associated with the edge, and the form shown in (8) indicates clearly how it can be distributed in a positive manner according to the direction of the local advection velocity, *i.e.*

$$S_1\,u_1 \;\;\rightarrow\;\; S_1\,u_1 + 3\Delta t\,[\widehat{\vec{\lambda}}_{12} \cdot \vec{n}]^- \,(u_1 - u_2)/2$$

$$S_2\,u_2 \;\;\rightarrow\;\; S_2\,u_2 + 3\Delta t\,[\widehat{\vec{\lambda}}_{12} \cdot \vec{n}]^+ \,(u_1 - u_2)/2$$

$$S_3\,u_3 \;\;\rightarrow\;\; S_3\,u_3 + 3\Delta t\,[\widehat{\vec{\lambda}}_{43} \cdot \vec{n}]^+ \,(u_4 - u_3)/2$$

$$S_4\,u_4 \;\;\rightarrow\;\; S_4\,u_4 + 3\Delta t\,[\widehat{\vec{\lambda}}_{43} \cdot \vec{n}]^- \,(u_4 - u_3)/2\,, \tag{10}$$

where $[\ ]^{\pm}$ signifies the positive/negative part of the quantity and $S_k\ (k = 1, 2, 3, 4)$ is the area of the mesh cell whose vertex is being updated. It is simple to make this edge distribution linearity preserving but this seems to have little effect on the numerical results.

Each mesh node now corresponds to many cell vertices and multiple values of u. When the new edge-based fluctuations are distributed along with the original cell-based fluctuations each u_i^j (the value associated with vertex i of cell j) receives contributions from precisely one cell and two edges (subject to the application of boundary conditions), leading to the update

$$(u_i^j)^{n+1} \;=\; (u_i^j)^n + \frac{3\Delta t}{S_j}\left(\alpha_i^j\,(\phi_c)_j + \alpha_i^{k_1}\,(\phi_e)_{k_1} + \alpha_i^{k_2}\,(\phi_e)_{k_2}\right), \tag{11}$$

in which the indices follow the annotation on the right hand side of Figure 1 and S_j is the area of cell j. The distribution coefficients for the edge fluctuations can be found easily from (8) and (10). Note that it is easy to show that the contribution due to degenerate polygon shown at the vertex in the centre of the right hand diagram in Figure 1 is zero.

The extension to nonlinear systems of equations of the form

$$\underline{U}_t + \vec{\nabla} \cdot \underline{\vec{F}} \;=\; \underline{0} \qquad \text{or} \qquad \underline{U}_t + \vec{\mathbf{A}} \cdot \vec{\nabla}\underline{U} \;=\; \underline{0}, \tag{12}$$

where $\vec{\mathbf{A}}$ represents the relevant flux Jacobians, with appropriate initial and boundary conditions on a domain Ω, is straightforward, assuming that conservative linearisation exists [3, 5]. The cell fluctuations (2)/(3) become

$$\underline{\Phi}_c \;=\; -\int_\triangle \vec{\nabla} \cdot \underline{\vec{F}} \, d\Omega \;=\; \oint_{\partial\triangle} \underline{\vec{F}} \cdot \vec{n} \, d\Gamma \;=\; -\int_\triangle \vec{\mathbf{A}} \cdot \vec{\nabla}\underline{U} \, d\Omega \;=\; -S_\triangle \widetilde{\vec{\mathbf{A}}} \cdot \widetilde{\vec{\nabla}\underline{U}} \tag{13}$$

and can be distributed as usual, using any of the standard methods for nonlinear systems [7]. The edge fluctuations (6)/(8) are now

$$\underline{\Phi}_e \;=\; \int_| [\underline{\vec{F}} \cdot \vec{n}] \, d\Gamma \;=\; \frac{1}{2} \widehat{\vec{\mathbf{A}}}_{12} \cdot \vec{n} \, (\underline{U}_1 - \underline{U}_2) \;+\; \frac{1}{2} \widehat{\vec{\mathbf{A}}}_{43} \cdot \vec{n} \, (\underline{U}_4 - \underline{U}_3), \tag{14}$$

in which $\widehat{\vec{\mathbf{A}}} = \vec{\mathbf{A}}(\hat{U})$ is defined using averages of the parameter vector variables [5] analogous to those shown for scalar advection in (9). The $\underline{\Phi}_e$ could easily be distributed directly, but to retain the positivity of the scalar schemes they are here decomposed using Roe's flux difference splitting [5], via the diagonalisation of the matrix given by $\widetilde{\vec{\mathbf{A}}} \cdot \vec{n} = \widetilde{\mathbf{R}}\, \widetilde{\mathbf{\Lambda}}\, \widetilde{\mathbf{R}}^{-1}$. Upwinding (and hence positivity) is applied using the wave speeds which appear in the diagonal eigenvalue matrix $\widetilde{\mathbf{\Lambda}}$. The resulting scheme is conservative, positive, linearity preserving, compact, upwind and continuous (when the underlying distributions are).

4. NUMERICAL EXPERIMENTS

Inviscid compressible fluid flow is simulated using the Euler equations. The test cases used involve flow from left to right through a channel of dimensions $[0, 3] \times [0, 1]$ with additional symmetric bumps situated on each wall giving a channel breadth of $b(x) = 1 - B\sin^2(\pi(x - 1))$ in the interval $x \in [1, 2]$ and $b(x) = 1$ elsewhere. Here $B = 0.1$ has been chosen with three freestream Mach numbers (M_∞) specified at inflow to give subcritical, transcritical and supercritical flows. The mesh used is a subdivision of a uniform 64×32 quadrilateral mesh in which the diagonals alternate their orientation. Figure 2 shows contours of density for each of the three cases and illustrates how the continuous and discontinuous schemes give similar results, though the latter appears to capture discontinuities more sharply. In each case the elliptic-hyperbolic wave decomposition model of Roe and Mesaros [4] was used for the cell fluctuations while Roe's flux difference splitting [5] was used for the edge fluctuations. Similar results have been achieved using matrix distribution schemes [7].
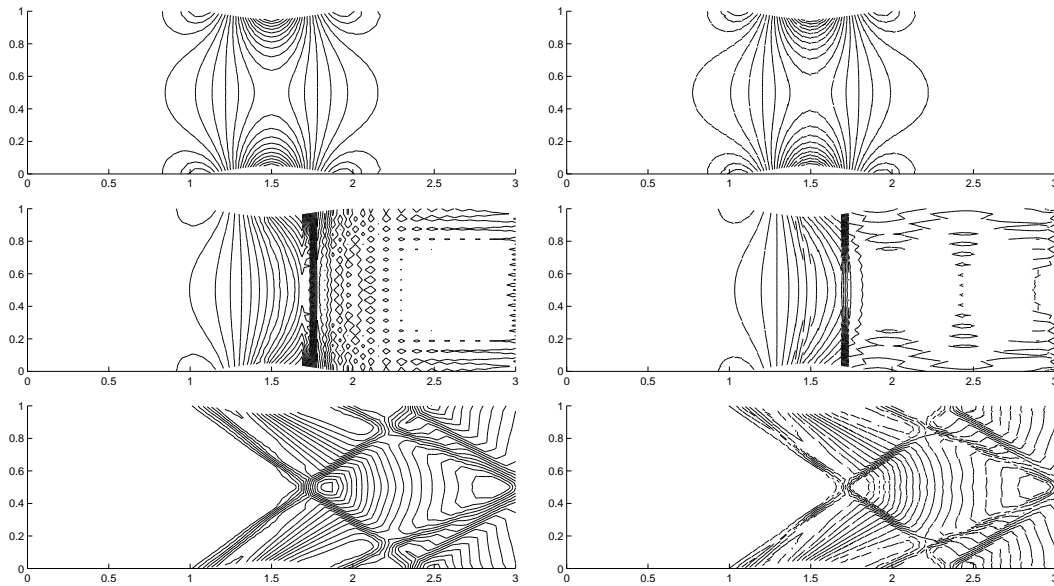
Figure 2. Flows through indented channels with $M_\infty = 0.5$ (subcritical flow – top), $M_\infty = 0.7$ (transcritical flow – middle) and $M_\infty = 2.0$ (supercritical flow – bottom) using continuous (left) and discontinuous (right) schemes.

5. CONCLUSIONS

A framework has been presented within which fluctuation distribution can be carried out when the underlying representation of the dependent variable is discontinuous. It has been successfully applied to a range of scalar conservation laws, and new results for the Euler equations of gasdynamics are presented here. Although there are many possible extensions, future research will initially focus on improving the rate of convergence to the steady state, increasing the scheme's accuracy (all of h-, p and r-adaptivity are possible), and applying the approach to time-dependent problems.

REFERENCES

1. Carette J-C, Deconinck H, Paillère H, Roe PL. Multidimensional upwinding: its relation to finite elements. *International Journal for Numerical Methods in Fluids* 1995;**20**(8-9):935–955.
2. Cockburn B. Discontinuous Galerkin methods for convection dominated problems. In *High-Order Methods for Computational Physics,* Barth TJ, Deconinck H (eds). Springer, 1999; 69–224.
3. Deconinck H, Roe PL, Struijs R. A multidimensional generalization of Roe's flux difference splitter for the Euler equations. *Computers and Fluids* 1993;**22**(2-3):215–222.
4. Mesaros LM, Roe PL. Multidimensional fluctuation splitting schemes based on decomposition methods. In *12th AIAA CFD Conference Proceedings*, 1995. Paper AIAA-95-1699.
5. Roe PL. Approximate Riemann solvers, parameter vectors and difference schemes. *Journal of Computational Physics* 1981;**43**(2):357–372.
6. Roe PL. Fluctuations and signals, a framework for numerical evolution problems. In *Numerical Methods for Fluid Dynamics*, Morton KW, Baines MJ (eds.). Academic Press, 1982; 219–257.
7. *High Order Discretization Methods,* VKI LS 2006–01, von Karman Institute for Fluid Dynamics, 2006.